

Regenerating evanescent waves from a silver superlens

Nicholas Fang, Zhaowei Liu, Ta-Jen Yen, and Xiang Zhang

Department of Mechanical and Aerospace Engineering, University of California at Los Angeles,

420 Westwood Plaza, Los Angeles, California 90095

xiang@seas.ucla.edu

<http://microlab.seas.ucla.edu>

Abstract: We investigated a precursor of superlensing: regenerating evanescent waves by excitation of a surface plasmon. Because the permittivity of a silver slab approaches -1 , we experimentally observed a broadening of surface-plasmon bandwidth. Our study identifies a means to access deep subwavelength features by use of a metamaterial superlens.

© 2003 Optical Society of America

OCIS codes: (110.2990) Image Formation Theory; (240.6690) Surface Waves; (260.3910) Optics of Metals

References and links

1. H. Kosaka, T. Kawashima, *et al.*, “Superprism phenomena in photonic crystals,” *Phys. Rev. B* **58**, R10096 (1998).
 2. D. Smith, W. Padilla, *et al.*, “Composite medium with simultaneously negative permittivity and permeability,” *Phys. Rev. Lett.* **84**, 4184-4187 (2000).
 3. V. Veselago, “The electrodynamics of substances with simultaneously negative ϵ and μ ,” *Sov. Phys. Usp.* **10**, 509-514 (1968).
 4. J. B. Pendry, “Negative refraction makes a perfect lens,” *Phys. Rev. Lett.* **85**, 3966-3969 (2000).
 5. S. A. Ramakrishna, J. B. Pendry, D. Schurig, D. R. Smith, and S. Schultz, “The asymmetric lossy near perfect lens,” *J. Mod. Opt.* **49**, 1747(2002).
 6. H. Raether, *Surface Plasmons* (Springer-Verlag, Berlin, 1988).
 7. P. B. Johnson and R. W. Christy, “Optical constants of the noble metals,” *Phys. Rev. B* **6**, 4370-4379 (1972).
 8. S. Hayashi, T. Kume, T. Amano, and K. Yamamoto, “A new method of surface plasmon excitation mediated by metallic nanoparticles,” *Jpn. J. Appl. Phys.* **35**, L331-L334 (1996).
 9. E. Kroeger and E. Kretschmann, “Scattering of light by slightly rough surfaces or thin films including plasma resonance emission,” *Z. Physik* **237**, 1-15 (1970).
 10. E. Kretschmann, “The angular dependence and the polarization of light emitted by surface plasmons on metals due to roughness,” *Opt. Commun.* **5**, 331-336 (1972).
 11. W. H. Weber and G. W. Ford, “Optical electric-field enhancement at a metal surface arising from surface plasmon excitation,” *Opt. Lett.* **6**, 122-124 (1981).
 12. Z. Liu, N. Fang, T.-J. Yen, and X. Zhang are preparing a manuscript to be called “Observation of rapid growth of evanescent wave with thickness of a negative permittivity slab: a key for superlens.”
-

1. Introduction

Metamaterials have opened an exciting gateway to achieving unprecedented physical properties and functionality unattainable from naturally existing materials. The “atoms” and “molecules” in metamaterials can be tailored in shape and size, the lattice constant and interatomic interaction can be artificially tuned, and “defects” can be designed and placed at desired locations. Pioneering research on strongly modulated photonic crystals [1] represents a giant step in engineering metamaterials. The recent discovery of left-handed metamaterials (LHMs) [2] is an example of a new exciting area in physics. A medium of this type [3] exhibits a unique negative refractive index in the design of negative effective permittivity and permeability simultaneously over certain frequency bands, and thus it is also termed a negative refractive-index medium (NRIM).

As recently observed by Pendry [4], the unique properties of NRIM allow a single slab of it to be used as a superlens, capable of focusing all Fourier components from the object onto a two-dimensional image with a resolution far below the diffraction limit. The key to the superlensing effect is the following: those waves that would normally decay away from the

object in free space or in a positive refractive-index material instead grow exponentially through the NRIM, compensating for the decay in the rest of optical path. This provides the possibility of reconstructing a diffraction-free image by collection of all Fourier components including these evanescent waves.

Here we experimentally demonstrate a key precursor for an optical superlens: regenerating an evanescent field at surface-plasmon resonance by use of a negative-permittivity silver film. We also examine the bandwidth requirement in restoring evanescent waves to achieve a superlens.

2. Theoretical background

Reference [4] indicates that for P -polarized light, a negative permittivity is sufficient for focusing evanescent waves, provided that film thickness and object and image distances are much smaller than the incident wavelength. To elucidate how a silver slab can mimic a NRIM at near field, we pick up an asymmetric configuration in which a thin film of silver is sandwiched between air and glass, and we investigate the transmissivity of the P -polarized evanescent waves across the silver layer.

For an evanescent wave with given k_x , we have $k_{zj} = +\left[\epsilon_j(\omega/c)^2 - k_x^2\right]^{1/2}$ for $j = 1$ (air) and $j = 3$ (glass); and $k_{z1} = +i\left[k_x^2 - \epsilon_1(\omega/c)^2\right]^{1/2}$ for $j = 2$ (silver). Given the thickness d of the silver slab, we can solve the overall transmission coefficient by using Fresnel equations:

$$T_p(k_x, d) = \frac{t_{12}t_{23}}{\exp(-ik_{z2}d) + r_{12}r_{23}\exp(+ik_{z2}d)}, \quad (1)$$

where

$$r_{12} = \frac{\frac{k_{z1} - k_{z2}}{\epsilon_1 - \epsilon_2}}{\frac{k_{z1} + k_{z2}}{\epsilon_1 + \epsilon_2}}, \quad r_{23} = \frac{\frac{k_{z2} - k_{z3}}{\epsilon_2 - \epsilon_3}}{\frac{k_{z2} + k_{z3}}{\epsilon_2 + \epsilon_3}},$$

and $t_{12} = 1 + r_{12}$, $t_{23} = 1 + r_{23}$.

To approximate an exponential growth of the overall transmission T_p , we will need the following condition $|r_{12}r_{23}| >> 1$ to be satisfied:

$$\left| \frac{k_{z1} - k_{z2}}{\epsilon_1 - \epsilon_2} \right| \left| \frac{k_{z2} - k_{z3}}{\epsilon_2 - \epsilon_3} \right| >> \left| \frac{k_{z1} + k_{z2}}{\epsilon_1 + \epsilon_2} \right| \left| \frac{k_{z2} + k_{z3}}{\epsilon_2 + \epsilon_3} \right|. \quad (2)$$

In an electrostatic limit, $k_{zj} = ik_x$, and inequality (2) is much simplified:

$$|\epsilon_2 - \epsilon_1||\epsilon_3 - \epsilon_2| >> |\epsilon_2 + \epsilon_1||\epsilon_3 + \epsilon_2|. \quad (3)$$

Assuming that both ϵ_1 and ϵ_3 are loss-free, we require

$$-\text{Re}(\epsilon_2)\left(|\epsilon_2|^2 + \epsilon_1\epsilon_3\right)(\epsilon_1 + \epsilon_3) > 0. \quad (4)$$

Inequality (4) clearly indicates the negative sign of ϵ_2 , whereas the permeability of the silver slab is not relevant.

Formula (2) provides a hint to understanding the superlensing effect: for regenerating the evanescent waves, we need to operate with the condition $\left| \frac{k_{z1}}{\varepsilon_1} + \frac{k_{z2}}{\varepsilon_2} \right| \left| \frac{k_{z2}}{\varepsilon_2} + \frac{k_{z3}}{\varepsilon_3} \right| \rightarrow 0$.

Physically, this would require exciting a surface plasmon at either the air or the glass side; a detailed analysis can be found in Refs. [5] and [6].

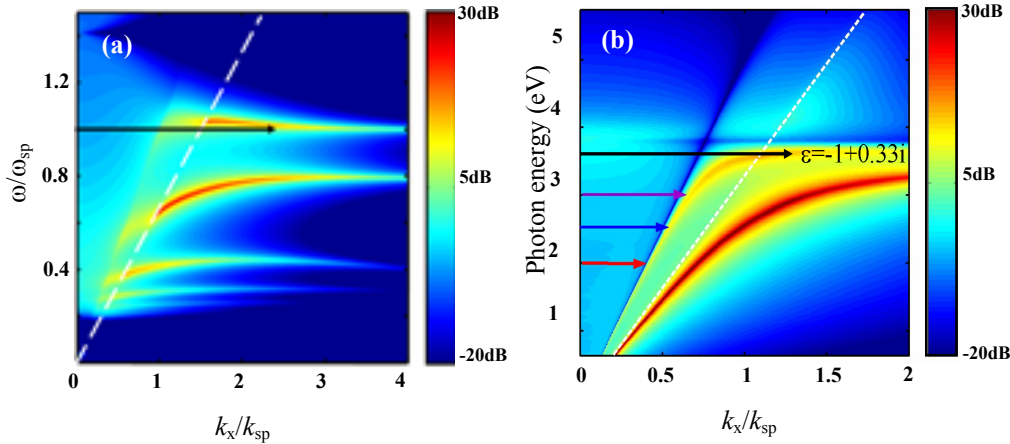


Fig. 1. Computed isotherm contour of transmissivity $|T_p|^2$ of (a) a conceptual NRIM slab and (b) a 50-nm silver film surrounded by air and glass ($n = 1.52$). In (a) $d = 0.14\lambda_{sp}$; $\varepsilon_2 = 1 - 2\omega_{sp}^2/(\omega^2 + 0.01i\omega_{sp})$, and $\mu_2 = 1 - 1.6\omega_{sp}^2/[(\omega - 0.106\omega_{sp})^2 + 0.01i\omega\omega_{sp}]$, $k_{sp} = \omega_{sp}/c$. In (b) the permittivity data are taken from Ref. [7].

An ideal perfect lens should allow amplification of evanescent waves for any k_x components. In other words, the permitted bandwidth of k_x for the enhancement of evanescent waves in the medium should extend to infinity [4]. However, in real situations, there exists finite bandwidth of k_x in which enhancement can be realized. To illustrate this, in Figs. 1(a) and 1(b) we plotted $|T_p|^2$ of a conceptual NRIM slab lens and a silver film as a function of photon energy and wave vector k_x . For both cases, at the photon energy where $\varepsilon(\omega) \rightarrow -1$, we can identify an enhanced transmissivity over a wide spectrum of evanescent waves. However, as we move away from this optimal wavelength, a pronounced transmissivity remains nearby the wave vector $k_x = (\omega/c)[\varepsilon_2(\mu_2 - \varepsilon_2)/(1 - \varepsilon_2^2)]^{1/2}$ [5]; and more specifically, in the case of a silver film, this dispersion relationship is well known: $k_x = +(\omega/c)[\varepsilon_2/(1 + \varepsilon_2)]^{1/2}$. Although many physical phenomena are to be explored experimentally at $\varepsilon(\omega) \rightarrow -1$, it is necessary to start with the investigation of a key precursor of superlensing: regenerating the evanescent waves along the dispersion curve of surface-plasmon resonance, because the concept provides a means of accessing the subwavelength information by future metamaterial superlenses.

3. Experiments and discussion

To experimentally quantify the allowed bandwidth for regenerating the evanescent waves at different photon energy, we constructed a reversed attenuated total-reflection (RATR) system that is similar to the one in Ref. [8], as shown in Fig. 2(a). With a programmable e-beam evaporator, a 50-nm-thick silver film was deposited on the flat surfaces of a semispherical glass prism with refractive index $n_p = 1.52$. Using a Dimension 3100 atomic force microscope (AFM), we characterized the surface roughness of the prism before and after deposition. The

roughness of the bare prism surface and the silver film is of the order of a few angstroms and a few nanometers, respectively. A collimated Ar⁺ laser beam (E field at the x direction, or polarization $\phi = 0^\circ$) with a wavelength λ (351.1–514.5 nm) and a diameter of <1.5 mm is incident normally on the center of a semispherical BK7 prism from the flat side. The mounted samples are leveled and centered with microactuators with 10-μm resolution. This step ensures a concentricity of better than 300 μm.

The coupling mechanism is shown in Fig. 2(b). Instead of placing a near-field object for the case of real superlens imaging, we now utilize the subwavelength surface roughness at the silver-air interface to scatter the incident beam to all possible k_x directions. The polarization current induced by the incoming electromagnetic field can be decomposed of three components in x , y , z , each acting as a Hertzian dipole on the metal surface. In the case of weak scattering from a smooth surface with small waviness [9], the scattered far-field light intensity dI per solid angle element $d\Omega$ normalized by incident intensity I_0 can be written as [10]

$$\frac{dI}{I_0 d\Omega} = 4 \left(\frac{\pi}{\lambda} \right)^4 |T_p(k_x, d)|^2 |S(k_x)|^2 |W(\theta, \phi)|^2, \quad (6)$$

with T_p being the p -polarization transmission coefficient of the evanescent field through the silver film, λ the incident wavelength, $|S(k_x)|$ the roughness Fourier spectrum of the silver-air interface, and $W(\theta, \phi)$ the dipole function. When the incident frequency is fixed, the photon impinging on the metal surface can excite the collective oscillation of conductive electrons at certain wave vectors, i.e., the surface plasmon with maximum efficiency. Therefore by coupling with a hemispherical prism in our case, we can see a transmitted hollow cone by use of a screen [Fig. 2(a)]. Note that the enhanced evanescent waves draw their power from the power of incoming light beams redistributed on the wavy surface; thus by explicitly applying the energy conservation, we also obtain Eq. (6) following an approach similar to that in Ref. [11].

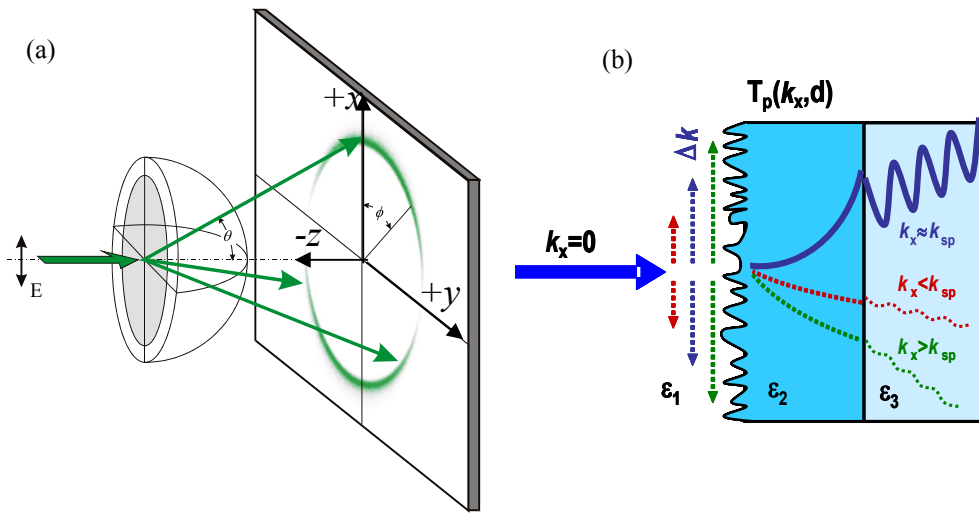


Fig. 2. (a) Schematic RATR setup. (b) Assumed evanescent coupling by surface roughness scattering.

According to Ref. [6], the internal scattering resulting from bulk inhomogeneities is far below the comparable level of surface roughness; thus in Eq. (6) we account for just one

occurrence of roughness scattering at the air–metal interface. This is verified by the $\phi = 90^\circ$ dips in the scattered cone, which excludes the polarization mixing that results from volume scattering. Therefore it is mainly the conversion to evanescent waves at the first surface that will be captured. Here we also assumed that the roughness at the metal–prism interface does not contribute to the collection of evanescent waves, because as we mentioned, the roughness that is due to the glass prism is 1 order of magnitude lower than that of air–metal surface.

An 8 mm \times 6 mm charge-coupled device (CCD) camera is placed \sim 5 cm from the center of the BK7 prism to measure the azimuthal angular distribution of relative light intensity near θ_{sp} (the surface-plasmon coupling angle), while ϕ is centered at zero. For further enhancing the intensity resolution, the intensity profiles captured by the CCD camera are averaged in the ϕ direction. The angular resolution and repeatability in the setup are calibrated to within 0.1° . The direct transmission at the center of the prism is blocked by a mask.

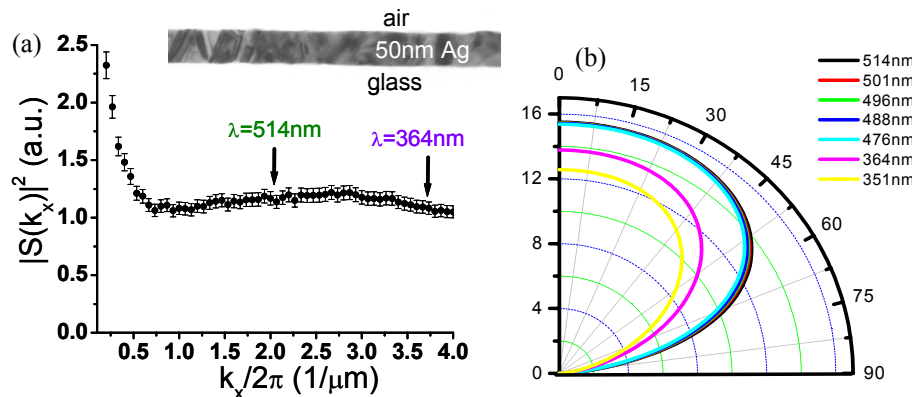


Fig. 3. (a) Fourier-transformed roughness spectrum of a 50-nm silver film as probed by AFM. Inset, a cross-sectional TEM picture of a 50-nm silver film for comparison. (b) Computed dipole function $|W(\theta,0)|^2$ as a function of scattered angle.

In a recent study [12], we quantitatively characterized the surface roughness of our sample with an AFM. After obtaining a two-dimensional Fourier transformation of the surface profile, we then averaged the radial roughness spectrum of the 50-nm silver sample as shown in Fig. 3(a). For comparison, in the inset of Fig. 3(a) we show a cross-sectional transmission electron micrograph (TEM) of a deposited 50-nm sample. The surface roughness characteristics as observed from the AFM and TEM are in good agreement (deviation of $<10\%$) at the wave vector k_x of interest, indicating an accuracy of $|S(k_x)|^2$. Figure 3(b) depicts the dipole function $|W(\theta,0)|^2$ (with a normal-incidence light source) as a function of the scattered angle for different incident wavelengths. From the results of Figs. 3(a) and 3(b), we then successfully extracted the enhanced transmissivity $|T_p|^2$ as a function of wavelength by using Eq. (6).

Finally, in Fig. 4(a), we show the transmissivity through a 50-nm-thick silver film for different incident wavelength. At $\lambda = 514$ nm, we find $|T_p|^2 > 1$ for a range of $\theta = 46^\circ$ – 49° , which corresponds to $k_x = 1.09$ – $1.15 k_0 (=2\pi/\lambda)$. By decreasing the wavelength λ from 514.5 to 351.1 nm [$\varepsilon(\omega) \rightarrow -1$], we can clearly observe a bandwidth broadening of amplified k spectrum accompanied by a remarkable shift of resonant peak toward larger angle θ as k_{sp} increases with decreasing $|\varepsilon|$. At $\lambda = 351$ nm, where $\varepsilon_{Ag} = -1.5 + 0.27i$, the bandwidth of the amplified evanescence wave spectrum approaching the full measurable range of $\frac{2\pi}{\lambda} < k_x \leq \frac{2\pi n_p}{\lambda}$ bounded by the light cones, or $k_x = 1.02$ – $1.48 k_0 (=2\pi/\lambda)$. The measured expansion of bandwidth is in good agreement with theoretical calculations in Fig. 1(b), which

provides a design base for improving the accessible bandwidth for the superlens imaging. To illustrate the broadening and shift of the resonant peak of evanescent waves, in Fig. 4(b) a naturally polarized white-light lamp is used to excite the surface plasmon of all wavelengths. A photograph of a true-color scattering image recorded on a diffusive screen is shown in Fig. 4(b). We can observe that the dispersion of the surface plasmon exhibited a rainbow-like pattern on the scattered ring; meanwhile, when the light turns to violet, the bandwidth apparently increases.

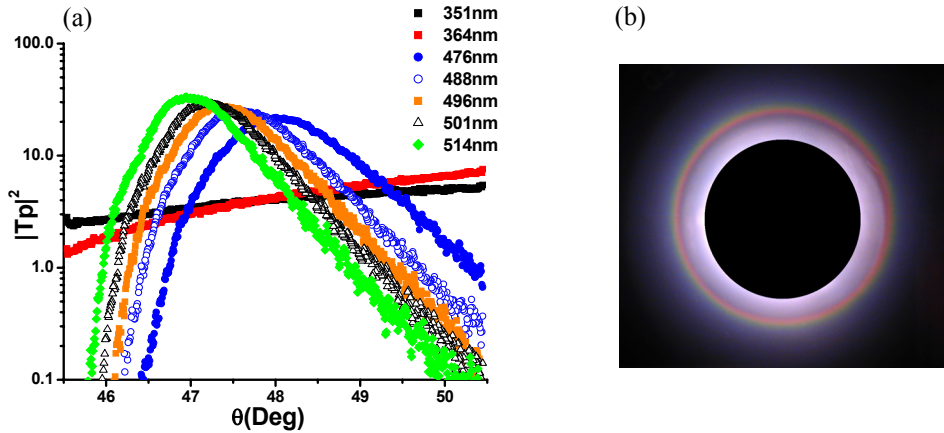


Fig. 4. (a) Azimuthal profile of the measured transmissivity of a 50-nm silver film for different light wavelengths. (b) Observed rainbow-like transmitted ring using a focused white-light source.

4. Conclusions

The foundation of superlensing theory—regeneration of evanescent waves by means of a metal film—has been validated in our experiment. Enhanced transmissivity of evanescent waves through a silver film is achieved by means of exciting them through natural surface roughness and analyzing the dipole radiation characteristics of the surface scatterers. The transmissivity bandwidth apparently broadens when the surface-plasmon excitation frequency approaches its resonance frequency. This opens the gateway to accessing the subwavelength features of a near-field object by synthesizing the enhanced evanescent components with the help of surface-plasmon excitation. Although these experiments are conducted with pristine silver films, the experimental configuration will provide a testbed for the artificially synthesized metamaterials.

On the other hand, to realize true far-field superresolution imaging, we have many challenges yet to solve. For example, a highly refined coupling mechanism is needed to convert a large band of these enhanced evanescent waves to propagating waves. With future metamaterials that allow broader k_x bandwidth to be coupled to the far field and with reduced loss, we are optimistic that the realization of a superlens will no longer be a dream.

Acknowledgments

The authors are grateful to S. A. Ramakrishna and J. B. Pendry of Imperial College and D. Smith and S. Schultz of UCSD for helpful discussions. This research has been supported by the MURI (Grant # N00014-01-1-0803), ONR (Grant # N00014-02-1-0224), and the NSF (Grant # DMII-9703426).